JOURNAL OF GUIDANCE, CONTROL, AND DYNAMICS
Vol. 20, No. 1, January–February 1997

Unification of Several System Realization Algorithms

Jer-Nan Juang*
NASA Langley Research Center, Hampton, Virginia 23681-0001

Unification of several system realization algorithms is presented using a generalized version of information matrix consisting of shifted input and output data correlations. The relationship of these realization algorithms is established using matrix factorization of the information matrix. The basis vectors of the column space and the null space of the information matrix are the key elements that provide the link among different realization algorithms. Frequency-domain versions of these realization algorithms are also introduced using the information matrix computed from the frequency response data. Experimental examples are given to illustrate the validity and usefulness of these algorithms with some comparison.

Nomenclature

A = state matrix, $n \times n$
B = input influence matrix, $n \times r$
C = output influence matrix, $m \times n$
D = direct transmission matrix, $m \times r$
$G(z_k)$ = frequency response function, $m \times r$, at the frequency variable z_k
I_i = identity matrix of order i
k = time index
ℓ = data length
m = number of outputs
n = order of the system
n_0 = number of zero singular values
$\mathcal{O}_p$ = observability matrix, $pm \times n$
p = integer determining the maximum order of the system
$\mathcal{R}, \bar{\mathcal{R}}$ = information matrix, $p(m+r) \times p(m+r)$
$\mathcal{R}_{hh}$ = fundamental system realization using information matrix correlation matrix, $pm \times pm$
$\mathcal{R}_{uu}$ = autocorrelation of shifted input data, $pr \times pr$
$\mathcal{R}_{uy}$ = cross-correlation of shifted input and output data, $pr \times pm$
$\mathcal{R}_{yy}$ = autocorrelation of shifted output data, $pm \times pm$
r = number of inputs
$\mathcal{U}$ = left singular matrix
$\mathcal{U}_n$ = columns of left singular matrix corresponding to nonzero singular values
$\mathcal{U}_0$ = columns of left singular matrix corresponding to zero singular values
$U_p(k)$ = output data matrix containing $\boldsymbol{u}(k)$ to $\boldsymbol{u}(k+p+N-2)$, $pm \times N$
$\boldsymbol{u}(k)$ = input force vector at time index k, $r \times 1$
$Y_p(k)$ = output data matrix containing $\boldsymbol{y}(k)$ to $\boldsymbol{y}(k+p+N-2)$, $pm \times N$
$\boldsymbol{y}(k)$ = output measurement vector at time index k, $m \times 1$
z_k = frequency-domain variable
α, β, Θ = parameter matrices
α_i = ith autoregressive exogeneous (ARX) coefficient matrix, $m \times m$, associated with output vector $\boldsymbol{y}(k+i)$
$\alpha(z_k)$ = ARX coefficient matrix, $m \times m$, associated with output vector $\boldsymbol{y}(z_k)$ at the frequency variable z_k
β_i = ith ARX coefficient matrix, $m \times r$, associated with input vector $\boldsymbol{u}(k+i)$
$\beta(z_k)$ = ARX coefficient matrix, $m \times r$, associated with input vector $\boldsymbol{u}(z_k)$ at the frequency variable z_k
Σ = singular value matrix
Σ_n = diagonal matrix containing nonzero singular values
Φ = working matrix
0_i = zero square matrix of order i
$0_{i \times j}$ = zero rectangular matrix of dimension i by j

Received March 11, 1996; revision received Oct. 8, 1996; accepted for publication Oct. 18, 1996.

*Principal Scientist, Structural Dynamics Branch. Fellow AIAA.

I. Introduction

THE area of system identification encompasses a multitude of approaches, perspectives, and techniques[1–15] whose interrelationships and relative merits are difficult to sort out. These techniques can be fundamentally divided into two groups. One group of techniques[1–13] uses the nonparametric approach to determine the input–output map using the least-squares method. The input–output map is characterized by a system model that may not have any physical meaning explicitly. These techniques are, in general, referred to as the black-box approach and are noniterative in nature. Basic mathematical foundations of the nonparametric identification theory are given in Ref. 1 showing the relationship among several different techniques in the time domain as well as the frequency domain. For modal parameter identification, Ref. 2 gives a framework to unify many existing estimation algorithms. Another group of techniques[15] uses the parametric approach to determine the parameters of a system model. The parameters may represent physical quantities such as the structural rigidity, mass inertia, etc. Optimization criteria are required to iteratively search for the optimal value of each parameter. As a result, nonlinear optimization techniques are involved in the computations. Both parametric and nonparametric approaches have their own merits with many successful applications. Therefore, it is difficult for a nonspecialist to extract the fundamental concepts upon which the two types of techniques are based. It may take considerable effort to gain enough understanding about a particular technique to be able to use it effectively in practice. While the development and enhancement of the many individual techniques continue, there is a need to provide a comprehensive yet coherent unification of the different techniques. In the past decade, researchers have successfully provided some frameworks to unify many different techniques via system realization theory.[1]

Many system realization algorithms start with a state-space discrete-time linear model and then formulate fundamental equations based on data correlation for computing system matrices. On the other hand, many other algorithms use the finite difference model and data correlation to solve for the system matrices. The two approaches appear to be fundamentally different due to their use of different types of models. This difference may yield the identification results with noticeable discrepancy because of the different equation errors that are minimized. As a result, it is very difficult for a user to interpret the identification results and choose the technique that is best suited for his problem. There is certainly a need to provide a comprehensive yet coherent unification of the different techniques.

Based on the mathematical framework developed for system realization using information matrix[12,13] (SRIM), the relationship among different realization techniques[1] is established. The SRIM is derived using the state-space discrete-time linear equation to form

a special form of data correlation for system realization. The other realization algorithms, such as the observer/Kalman filter identification (OKID)[10,11] technique, start with computing the coefficient matrices of the finite difference equation. The computation also requires information regarding input and output data correlation. The similarity of using data correlation leads naturally to establishing the relationship between the SRIM and the OKID method. Mathematical formulation will be given in detail to show how the different algorithms may be derived from the information matrix. The basis vectors of the column space and the null space of the information matrix are the key elements that provide the link among the different realization algorithms. Matrix factorization of the information matrix will be seen to be the most important step in the theoretical development and computational procedure to make possible the unification of the many different techniques. The approach presented here provides a way to better understand and interpret other techniques such as the subspace identification approach.[7–9]

The later part of the paper introduces the information matrix in the frequency domain. The information matrix computed from frequency response data will be shown to have the same characteristics as that obtained from the input–output data. That establishes the frequency-domain versions of SRIM and OKID and their relationship.

II. Time-Domain Methods

A deterministic linear time-invariant system is commonly represented by the following discrete-time state-space model[1]:

$$\boldsymbol{x}(k+1) = A\boldsymbol{x}(k) + B\boldsymbol{u}(k) \qquad \boldsymbol{y}(k) = C\boldsymbol{x}(k) + D\boldsymbol{u}(k) \quad (1)$$

where $\boldsymbol{x}(k)$ is an $n \times 1$ state vector at time index k, $\boldsymbol{u}(k)$ is an $r \times 1$ input vector corresponding to r inputs, and $\boldsymbol{y}(k)$ is an $m \times 1$ output vector associated with m sensor measurements. The system matrices A, B, C, and D with appropriate dimensions are unknown to be determined from given input and output data, i.e., $\boldsymbol{u}(k)$ and $\boldsymbol{y}(k)$ for $k = 0, 1, 2, \ldots, \ell$. Equation (1) describes the input and output relationship through the state vector $\boldsymbol{x}(k)$.

On the other hand, the input and output relationship may be described by the finite difference model. The finite difference model is commonly called the autoregressive exogeneous (ARX) model in the controls community. The discrete-time ARX model is typically written as

$$\begin{aligned}\alpha_{p-1}\boldsymbol{y}(k+p-1) + \alpha_{p-2}\boldsymbol{y}(k+p-2) + \cdots + \alpha_0\boldsymbol{y}(k) \\ = \beta_{p-1}\boldsymbol{u}(k+p-1) + \beta_{p-2}\boldsymbol{u}(k+p-2) + \cdots + \beta_0\boldsymbol{u}(k)\end{aligned} \quad (2)$$

where α_i, for $i = 0, 1, 2, \ldots, p-1$, is an $m \times m$ matrix; β_i, for $i = 0, 1, 2, \ldots, p-1$, is an $m \times r$ matrix; $\boldsymbol{y}(k)$ is an $m \times 1$ output vector at the time step k, and $\boldsymbol{u}(k)$ is an $r \times 1$ input vector at the time step k. This equation relates the output sequence $\boldsymbol{y}(k)$ to the input sequence $\boldsymbol{u}(k)$ up to p time steps with the absence of the state vector $\boldsymbol{x}(k)$ defined in Eq. (1). The ARX coefficient matrices can be computed from input and output data by minimizing the output equation error,[10] i.e., the error between the actual output and the estimated output.

Equation (2) produces the following matrix equality:

$$\alpha Y_p(k) = \beta U_p(k) \quad (3)$$

where

$$\alpha = \begin{bmatrix}\alpha_0 & \alpha_1 & \cdots & \alpha_{p-1}\end{bmatrix} \qquad \beta = \begin{bmatrix}\beta_0 & \beta_1 & \cdots & \beta_{p-1}\end{bmatrix}$$

$$Y_p(k) = \begin{bmatrix} \boldsymbol{y}(k) & \boldsymbol{y}(k+1) & \cdots & \boldsymbol{y}(k+N-1) \\ \boldsymbol{y}(k+1) & \boldsymbol{y}(k+2) & \cdots & \boldsymbol{y}(k+N) \\ \vdots & \vdots & \ddots & \vdots \\ \boldsymbol{y}(k+p-1) & \boldsymbol{y}(k+p) & \cdots & \boldsymbol{y}(k+p+N-2) \end{bmatrix} \quad (4)$$

$$U_p(k) = \begin{bmatrix} \boldsymbol{u}(k) & \boldsymbol{u}(k+1) & \cdots & \boldsymbol{u}(k+N-1) \\ \boldsymbol{u}(k+1) & \boldsymbol{u}(k+2) & \cdots & \boldsymbol{u}(k+N) \\ \vdots & \vdots & \ddots & \vdots \\ \boldsymbol{u}(k+p-1) & \boldsymbol{u}(k+p) & \cdots & \boldsymbol{u}(k+p+N-2) \end{bmatrix}$$

Let us define the following quantities:

$$\begin{aligned}\mathcal{R}_{yy} &= (1/N)Y_p(k)Y_p^T(k) \\ \mathcal{R}_{yu} &= (1/N)Y_p(k)U_p^T(k) \\ \mathcal{R}_{uu} &= (1/N)U_p(k)U_p^T(k)\end{aligned} \quad (5)$$

where $N = \ell - p$ with ℓ being the data length and p the data shift to form the data matrices $U_p(k)$ and $Y_p(k)$. The quantities $\mathcal{R}_{yy}$ and $\mathcal{R}_{uu}$ are symmetric matrices. The square matrices $\mathcal{R}_{yy}$ $(mp \times mp)$ and $\mathcal{R}_{uu}$ $(rp \times rp)$ are the autocorrelations of the output data $\boldsymbol{y}$ with time shifts and the input data $\boldsymbol{u}$ with time shifts, respectively. The rectangular matrices $\mathcal{R}_{yu}$ $(mp \times rp)$ represent the cross correlations of the output data $\boldsymbol{y}$ and input data $\boldsymbol{u}$. When the integer N is sufficiently long, the quantities defined in Eq. (5) approximate expected values in the statistical sense if the input and output data are stationary processes satisfying the ergodic property.

Postmultiplying Eq. (3) by $U_p^T(k)$ and noting Eq. (5) for definitions of $\mathcal{R}_{yu}$ and $\mathcal{R}_{uu}$ yield

$$\alpha\mathcal{R}_{yu} = \beta\mathcal{R}_{uu} \quad \Rightarrow \quad \beta = \alpha\mathcal{R}_{yu}\mathcal{R}_{uu}^{-1} \quad (6)$$

Here, the existence of $\mathcal{R}_{uu}^{-1}$ is assumed. Similarly, postmultiplying Eq. (3) by $Y_p^T(k)$ and noting Eq. (5) for definitions of $\mathcal{R}_{yy}$ and $\mathcal{R}_{yu}$ yield

$$\alpha\mathcal{R}_{yy} = \beta\mathcal{R}_{yu}^T \quad (7)$$

Substituting Eq. (6) for β into Eq. (7) thus gives

$$\alpha\left[\mathcal{R}_{yy} - \mathcal{R}_{yu}\mathcal{R}_{uu}^{-1}\mathcal{R}_{yu}^T\right] = 0$$

or

$$\alpha\mathcal{R}_{hh} = 0_{m \times pm} \quad (8)$$

where $0_{m \times pm}$ is an $m \times pm$ zero matrix and

$$\mathcal{R}_{hh} = \mathcal{R}_{yy} - \mathcal{R}_{yu}\mathcal{R}_{uu}^{-1}\mathcal{R}_{yu}^T \quad (9)$$

Equations (6) and (8) can be used for computing α and β.

Another way of computing α and β is to combine Eqs. (6) and (7) to yield

$$[-\alpha \quad \beta]\begin{bmatrix}\mathcal{R}_{yy} & \mathcal{R}_{yu} \\ \mathcal{R}_{yu}^T & \mathcal{R}_{uu}\end{bmatrix} = 0_{m \times p(m+r)} \quad (10)$$

or

$$\Theta\mathcal{R} = 0_{m \times p(m+r)} \quad (11)$$

where $0_{m \times p(m+r)}$ is an $m \times p(m+r)$ zero matrix and

$$\Theta = [-\alpha \quad \beta] \qquad \text{and} \qquad \mathcal{R} = \begin{bmatrix}\mathcal{R}_{yy} & \mathcal{R}_{yu} \\ \mathcal{R}_{yu}^T & \mathcal{R}_{uu}\end{bmatrix} \quad (12)$$

The size of matrix Θ is $m \times p(m+r)$, whereas the size of $\mathcal{R}$ is $p(m+r) \times p(m+r)$. The matrix $\mathcal{R}$ is called the information matrix consisting of shifted input and output data correlations. Equation (11) implies that the unknown matrix Θ lies in the column null space of the matrix $\mathcal{R}$. Any m columns generated from the basis vectors of the column null space of $\mathcal{R}$ may be considered as the solution for Θ^T. In theory, the integer p must be chosen large enough so that the $p(m+r) \times p(m+r)$ matrix $\mathcal{R}$ is rank deficient. Because the $pr \times pr$ input correlation matrix $\mathcal{R}_{uu}$ is required to have the full rank of pr, the rank deficiency of $\mathcal{R}$ implies that the rank of $\mathcal{R}_{yy}$ must be less than pm. To be specific, the rank of $\mathcal{R}_{yy}$ cannot be more than $pm - m$ to have at least m independent columns to generate the column null space of $\mathcal{R}$ of dimension m.

Based on the definition of the information matrix shown in Eq. (12), the relationship among several realization methods can be established using Eqs. (8) and (11). Three methods will be discussed including SRIM,[12] OKID,[10] and subspace model identification (SMI) schemes.[7–9]

A. SRIM Algorithm

The SRIM[12] is a realization algorithm to identify a discrete-time model directly from input and output data. The matrix $\mathcal{R}_{hh}$ shown in Eq. (9) is the one used by SRIM to compute the state matrix and the output matrix.

The approach used to derive SRIM starts with the discrete-time state-space model, Eq. (1), and proves that[12]

$$\mathcal{R}_{hh} = \mathcal{O}_p \tilde{\mathcal{R}}_{xx} \mathcal{O}_p^T \tag{13}$$

where

$$\mathcal{O}_p = \begin{bmatrix} C \\ CA \\ CA^2 \\ \vdots \\ CA^{p-1} \end{bmatrix} \tag{14}$$

is an observability matrix with A and C being the system state matrix and the output matrix, respectively. The matrix $\tilde{\mathcal{R}}_{xx}$ is a symmetric matrix, which reduces the correlation matrix of the state vector $\boldsymbol{x}$ when the current and future input data are uncorrelated with the current state.

From Eq. (13), it is clear that one may take a singular value decomposition to factor the matrix $\mathcal{R}_{hh}$ into the product of three matrices. Taking the singular value decomposition of the symmetric matrix $\mathcal{R}_{hh}$ yields

$$\mathcal{R}_{hh} = \mathcal{U}\Sigma^2\mathcal{U}^T = [\mathcal{U}_n \quad \mathcal{U}_0] \begin{bmatrix} \Sigma_n^2 & 0_{n\times n_0} \\ 0_{n_0\times n} & 0_{n_0} \end{bmatrix} \begin{bmatrix} \mathcal{U}_n^T \\ \mathcal{U}_0^T \end{bmatrix} = \mathcal{U}_n \Sigma_n^2 \mathcal{U}_n^T \tag{15}$$

The integer $n_0 = pm - n$ is the number of dependent columns in $\mathcal{R}_{hh}$, and $0_{n\times n_0}$ is an $n \times n_0$ zero matrix and 0_{n_0} is a square zero matrix of order n_0. The $pm \times n$ matrix $\mathcal{U}_n$ corresponds to the n nonzero singular values in the diagonal matrix Σ_n, whereas the $pm \times n_0$ matrix $\mathcal{U}_0$ is associated with the n_0 zero singular values. The matrix $\mathcal{U}_n$ can be treated as the observability matrix $\mathcal{O}_p$ that can be used to compute the state matrix A and the output matrix C. With A and C computed, the input matrix B and the direct transmission matrix D can be determined using any of the three methods shown in Ref. 12. The three methods are the indirect method, the direct method, and the output-minimization method.

B. OKID Algorithm

The OKID is a realization algorithm that can be used to determine a discrete-time model and its corresponding state observer. The ARX coefficient matrices α and β are computed and used to calculate the system Markov parameters and the observer gain Markov parameters. Both type of Markov parameters are then decomposed to realize the system matrices and the observer gain matrix.

Equation (8) implies that the $m \times pm$ parameter matrix α is in the column null space of the $pm \times pm$ matrix $\mathcal{R}_{hh}$. Any m rows of $\mathcal{U}_0^T$ from Eq. (15) may be used to construct the matrix α, i.e.,

$$\alpha = \text{ any } m \text{ rows of } \mathcal{U}_0^T \tag{16}$$

From Eq. (6), the $m \times pr$ matrix β can be solved by

$$\beta = \text{ any } m \text{ rows of } \mathcal{U}_0^T \mathcal{R}_{yu} \mathcal{R}_{uu}^{-1} \tag{17}$$

In practice, there may not exist any zero singular value to form the matrix $\mathcal{U}_0$ due to system uncertainties, including input and output noises. One may then select the m columns corresponding to the m smallest singular values to form $\mathcal{U}_0$.

Similar to Eq. (15), one obvious solution for Eq. (11) is to take the singular value decomposition of $\mathcal{R}$ and use the column vectors corresponding to the zero singular values as shown in Eq. (16) to determine α and β simultaneously. Another solution for Eq. (11) can be derived as follows. Let Eq. (11) be premultiplied by the $m \times m$ matrix α_{p-1}^{-1} to have

$$\alpha_{p-1}^{-1} \Theta \mathcal{R} = 0_{m\times p(m+r)} \tag{18}$$

or, from Eqs. (4) and (12),

$$\begin{bmatrix} -\alpha_{p-1}^{-1}\alpha_0 & -\alpha_{p-1}^{-1}\alpha_1 & \cdots & -I_m & \alpha_{p-1}^{-1}\beta_0 & \alpha_{p-1}^{-1}\beta_1 \\ & & & & \cdots & \alpha_{p-1}^{-1}\beta_{p-1} \end{bmatrix} \mathcal{R} = 0_{m\times p(m+r)}$$

Now, take out the m rows of $\mathcal{R}$ from $(p-1)\times m + 1$ to pm and move them to the right-hand side of Eq. (18), i.e.,

$$\tilde{\Theta} \begin{bmatrix} \mathcal{R}[1:(p-1)m, :] \\ \mathcal{R}[pm+1:(p+r)m, :] \end{bmatrix} = \mathcal{R}[(p-1)m+1:pm, :] \tag{19}$$

where

$$\tilde{\Theta} = \begin{bmatrix} -\alpha_{p-1}^{-1}\alpha_0 & -\alpha_{p-1}^{-1}\alpha_1 & \cdots & -\alpha_{p-1}^{-1}\alpha_{p-2} & \alpha_{p-1}^{-1}\beta_0 \\ & & & \alpha_{p-1}^{-1}\beta_1 & \cdots & \alpha_{p-1}^{-1}\beta_{p-1} \end{bmatrix} \tag{20}$$

Here, $\mathcal{R}[1:(p-1)m, :]$ is defined as the matrix consisting of the first $(p-1)m$ rows and all columns of $\mathcal{R}$. Similarly, $\mathcal{R}[pm+1:(p+r)m, :]$ is defined as the matrix formed from the $(pm+1)$th row to the $[(p+r)m]$th row and all columns of $\mathcal{R}$. Note that the dimension of $\tilde{\Theta}$ is $m \times [(p-1)m+pr]$, which is m columns shorter than Θ due to the removal of the identity matrix I_m. Equation (19) should have the least-squares solution for $\tilde{\Theta}$, i.e.,

$$\tilde{\Theta} = \mathcal{R}[(p-1)m+1:pm, :] \begin{bmatrix} \mathcal{R}[1:(p-1)m, :] \\ \mathcal{R}[pm+1:(p+r)m, :] \end{bmatrix}^{\dagger} \tag{21}$$

where $\dagger$ indicates pseudoinverse. To avoid the pseudoinverse, one may delete m columns of $\mathcal{R}[(p-1)m+1:pm, :]$ from $(p-1)m+1$ to pm, and corresponding m columns of

$$\begin{bmatrix} \mathcal{R}[1:(p-1)m, :] \\ \mathcal{R}[pm+1:(p+r)m, :] \end{bmatrix}$$

The parameter matrix $\tilde{\Theta}$ obtained from Eq. (21) is identical to the one used by the OKID[1,10] technique to identify system matrices A, B, C, and D and an observer gain G. In theory, all methods that start with the same correlation matrix $\mathcal{R}$ should produce the same identification results. In practice, the identification results may be somewhat different due to the presence of system uncertainties. For example, the matrix $\tilde{\Theta}$ solved by Eq. (21) minimizes the output residual between the measured output and the ARX computed output.[1,10] On the other hand, some other methods[7–9] minimize the error between the measured output and the output computed from an identified state-space model. Because different error criteria are used for minimization, results are expected to be somewhat different. Nevertheless, the results should not be significantly different unless the identified models are considerably reduced by either singular values truncation and/or modal truncation.

C. SMI Algorithms

The main characteristic of SMI[7–9] algorithms is the calculation of specially structured subspaces of spaces defined by the Hankel matrix consisting of input and output data. This structure is then exploited in the computation of a system realization. The common feature is their algorithmic organization: a QR factorization followed by a singular value decomposition and the solution of an overdetermined set of equations.

Because the data matrices $Y_p(k)$ and $U_p(k)$ are the only information given, one may focus on these two matrices to extract other information necessary to determine the system matrices A, B, C, and D. Let $H_p(k)$ be the Hankel matrix defined by

$$H_p(k) = \begin{bmatrix} U_p(k) \\ Y_p(k) \end{bmatrix} \tag{22}$$

which may be decomposed by the QR factorization such that

$$\begin{bmatrix} U_p(k) \\ Y_p(k) \end{bmatrix} = H_p(k) = RQ = \begin{bmatrix} R_1 & 0_{pr\times pm} \\ R_{21} & R_2 \end{bmatrix} \begin{bmatrix} Q_1 \\ Q_2 \end{bmatrix} \tag{23}$$

where $0_{pr\times pm}$ is a $pr \times pm$ zero matrix. The Q matrix is partitioned into two submatrices Q_1 of dimension $pr \times N$ and Q_2 of dimension

$pm \times N$. Similarly, R is partitioned into four submatrices R_1 of dimension $pr \times pr$, R_{21} of dimension $pm \times pr$, R_2 of dimension $pm \times pm$, and $0_{pr \times pm}$. Since the matrix Q in the QR factorization is orthonormal, it satisfies

$$Q_1 Q_1^T = I_{pr}, \qquad Q_2 Q_1^T = 0_{pm \times pr}, \qquad Q_2 Q_2^T = I_{pm} \tag{24}$$

where I_{pr} is an identity matrix of order pr, I_{pm} is an identity matrix of order pm, and $0_{pm \times pr}$ is a zero matrix of dimension $pm \times pr$. The matrix $R_y(k)$ has been proven, in Ref. 8, to have the following property:

$$R_2 = \mathcal{O}_p X \tag{25}$$

where $\mathcal{O}_p$ is the observability matrix defined in Eq. (14) and X is an $n \times pm$ matrix. The SMI[8] starts with the QR factorization of the $p(r+m) \times N$ Hankel matrix shown in Eq. (22) to compute the matrix R_2 and then take the singular value decomposition of R_2 to obtain the left singular matrix, i.e., the observability matrix $\mathcal{O}_p$. The observability matrix $\mathcal{O}_p$ is then used to compute the state matrix A and the output matrix C. With A and C given, the input influence matrix B and the direct transmission matrix D are then computed by minimizing the output error.

Equation (23) clearly implies that

$$U_p(k) = R_1 Q_u \qquad Y_p(k) = R_{21} Q_u + R_2 Q_y \tag{26}$$

From Eqs. (22) and (23), it is easy to show that

$$H_p(k) H_p^T(k) = \begin{bmatrix} U_p(k)U_p^T(k) & Y_p(k)U_p^T(k) \\ Y_p(k)U_p^T(k) & Y_p(k)Y_p^T(k) \end{bmatrix} = \begin{bmatrix} R_1 R_1^T & R_1 R_{21}^T \\ R_{21} R_1^T & R_{21} R_{21}^T + R_2 R_2^T(k) \end{bmatrix} \tag{27}$$

where Eq. (24) has been used to arrive at Eq. (27). Equation (27) provides the equalities

$$R_1 R_1^T = U_p(k) U_p^T(k) \tag{28}$$

$$R_{21} R_1^T = Y_p(k) U_p^T(k) \Rightarrow R_{21} = Y_p(k) U_p^T(k) \left[R_1^T\right]^{-1} \tag{29}$$

$$\begin{aligned} R_2 R_2^T(k) &= Y_p(k) Y_p^T(k) - R_{21} R_{21}^T \\ &= Y_p(k) Y_p^T(k) - Y_p(k) U_p^T(k) \left[R_1^T\right]^{-1} [R_1]^{-1} U_p(k) Y_p^T(k) \end{aligned} \tag{30}$$

which, with the substitution of Eq. (28) into Eq. (30), lead to

$$\begin{aligned} R_2 R_2^T(k) &= Y_p(k) Y_p^T(k) - Y_p(k) U_p^T(k) \\ &\quad \times \left[U_p(k) U_p^T(k)\right]^{-1} U_p(k) Y_p^T(k) \\ &= N\left(\mathcal{R}_{yy} - \mathcal{R}_{yu} \mathcal{R}_{uu}^{-1} \mathcal{R}_{yu}^T\right) \\ &= N \mathcal{R}_{hh} \end{aligned} \tag{31}$$

where Eqs. (5) and (26) have been used to obtain the last two equalities. The matrices R_2 and $\mathcal{R}_{hh}$ are not necessarily related uniquely. In other words, the square root of the matrix $N\mathcal{R}_{hh}$ does not necessarily produce the matrix R_2 (Ref. 16).

The SMI uses the matrix R_2 to compute the observability matrix $\mathcal{O}_p$ whereas the SRIM uses the matrix $\mathcal{R}_{hh}$ to produce $\mathcal{O}_p$. The SMI requires an QR factorization of a large matrix $H_p(k)$ followed by a singular value decomposition and the solution of an overdetermined set of equations. The SRIM algorithm incorporating the recursive formula[12] for computing the data correlation $\mathcal{R}_{hh}$ is more efficient computationally than SMI. With the absence of system uncertainties, both SRIM and SMI should produce the same identification results. In practice, significant discrepancy in identification results may occur due to considerable input and output noise, and numerical errors from factoring a large matrix.

D. Experimental Example

The experimental results given in this section illustrate the usefulness of the various realization techniques in practice. Figure 1 shows the truss structure used. The L-shaped structure consists of nine bays on its vertical section, and one bay on its horizontal section, extending 90 and 20 in., respectively.

The shorter section is clamped to a steel plate, which is rigidly attached to the wall. The square cross section is 10 × 10 in. Two cold air jet thrusters, located at the beam tip, serve as actuators for excitation and control. Each thruster has a maximum thrust of 2.2 lb. Two servo accelerometers located at a corner of the square cross-section provide the in-plane tip acceleration measurements. In addition, an offset weight of 30 lb is added to enhance the dynamic coupling between the two principal axes and to lower the structure fundamental frequency. For identification, the truss is excited using random inputs to both thrusters. The input–output signals are sampled at 250 Hz and recorded for system identification. A data record of 2000 points is used for identification.

The initial index p is arbitrarily set as shown in Table 1 to make the maximum system order, $pm = 10, 20, 30, 40, 50, 100$, and 200. Table 1 also lists the modal frequencies and damping ratios identified using the SRIM algorithm[12] without singular value (SV) truncation of $\mathcal{R}_{hh}$. The full-size A and C computed from $\mathcal{R}_{hh}$ are then reduced to order 6, including only those modes of interest. For the purpose of comparison, both the indirect method (IDM) and the output-error minimization (OEM) method are used for computing B and D with given reduced size A and C. The reduced model represented by A, B, C, and D is used to compute the output error. The last two columns in Table 1, Error max SV, give the largest SV of the error matrix between the real output and the output reconstructed from the identified system matrices using the same input signal. The error matrix is $m \times \ell$ where m is the number of outputs and ℓ the length of the data. As shown in Table 1, the OEM output error decreases quickly when p increases from 5 to 10 and reaches a minimum at $p = 15$. It increases slightly again and then reduces to another minimum at $p = 100$. The frequencies identified for all different p are very close whereas the damping ratios range from 3.5 to 0.4% for the first mode, from 2.3 to 0.45% for the second mode, and from 1.13 to 0.3% for the third mode.

Table 1 SRIM-identified modal parameters with modal truncation

	Mode 1		Mode 2		Mode 3		IDM	OEM
p	Freq (Hz)	Damp (%)	Freq (Hz)	Damp (%)	Freq (Hz)	Damp (%)	Error max SV	Error max SV
5	5.89	3.50	7.28	2.30	49.0	1.13	817.99	735.99
10	5.87	0.65	7.29	0.47	48.6	0.74	262.81	202.84
15	5.85	0.40	7.28	0.41	48.6	0.46	197.32	171.33
20	5.85	0.37	7.28	0.41	48.7	0.44	216.79	174.46
25	5.85	0.38	7.28	0.42	48.7	0.64	203.56	174.06
50	5.85	0.38	7.28	0.44	48.6	0.47	198.69	175.11
100	5.85	0.40	7.28	0.45	48.5	0.30	194.58	174.02

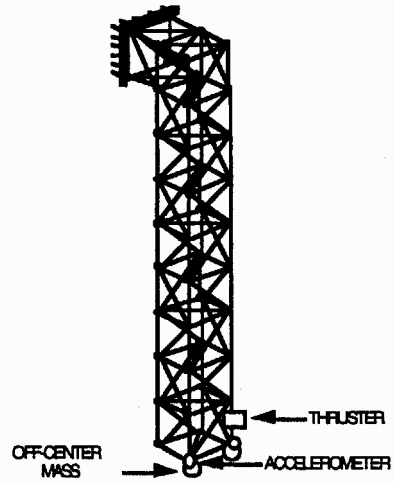

Fig. 1 Truss structure test configuration.

Table 2 OKID-identified modal parameters with modal truncation

	Mode 1		Mode 2		Mode 3		OKID	OEM
p	Freq (Hz)	Damp (%)	Freq (Hz)	Damp (%)	Freq (Hz)	Damp (%)	Error max SV	Error max SV
5	5.89	3.50	7.28	2.30	49.0	1.13	818.05	735.99
10	5.87	0.65	7.29	0.47	48.6	0.74	262.81	202.84
15	5.85	0.40	7.28	0.41	48.6	0.46	197.22	171.33
20	5.85	0.37	7.28	0.41	48.7	0.44	215.97	174.46
25	5.85	0.38	7.28	0.42	48.7	0.64	203.21	174.06
50	5.85	0.38	7.28	0.44	48.6	0.47	196.70	175.10
100	5.85	0.40	7.28	0.45	48.5	0.30	882.26	174.02

The same set of data from the truss structure shown in Fig. 1 is used. Now, the OKID method[10] is applied to determine the system matrices A, B, C, and D. Two computational steps are required. The first step is to use Eq. (21) to compute ARX coefficient matrices for determination of system Markov parameters (pulse response). The second step is to use the eigensystem realization algorithm[1] (ERA) from the computed pulse response to realize A, B, C, and D, simultaneously. In this example, no SV truncation is performed in ERA. The ERA-identified full-size model is then reduced to order 6, including only the modes of interest. The reduced model is then used to compute the output error.

Table 2 shows the modal frequencies and damping ratios identified using the OKID method. The output error decreases quickly when p increases from 5 to 10 and reaches a minimum at $p = 15$. It increases slightly again and then reduces to another minimum at $p = 50$. Tables 1 and 2 have identical modal parameters. The output errors in both tables are very close except at $p = 100$, where the value 882.26 in Table 2 is 4.5 times larger than 194.58 in Table 1. Since the modal parameters are identical in both tables, the error from C, B, and D may be the cause of the discrepancy. Indeed, when B and D are recomputed by the OEM method, the output error is brought back to the same level in both tables.

III. Frequency-Domain Methods

There are cases in which frequency response data rather than time histories are available. This is often the case with the advent of sophisticated spectrum analyzers. It is known that most time-domain methods have their frequency-domain counterparts.[1,2,14] In this section, we focus on the calculation of the information matrix from frequency response data.

Taking the z transform of the time-domain ARX model produces the frequency-domain ARX model. The coefficient matrices of the frequency-domain ARX model can be obtained from the frequency response data by minimizing the error between the real transfer function and the estimated transfer function at frequency points of interest. In theory, the ARX coefficient matrices obtained from the frequency-domain approach should be identical to those from the time-domain approach.

Let $G(z_k)$ be the transfer function matrix of the system described by Eq. (2). Consider the left matrix-fraction[1]

$$G(z_k) = \alpha^{-1}(z_k)\beta(z_k) \tag{32}$$

where

$$\begin{aligned}\alpha(z_k) &= \alpha_0 + \alpha_1 z_k^{-1} + \cdots + \alpha_{p-1} z_k^{-(p-1)} \\ \beta(z_k) &= \beta_0 + \beta_1 z_k^{-1} + \cdots + \beta_{p-1} z_k^{-(p-1)}\end{aligned} \tag{33}$$

are matrix polynomials. Every α_i is an $m \times m$ real square matrix and each β_i is an $m \times r$ real rectangular matrix. If $G(z_k)$ represents the frequency response function (FRF) obtained from experiments, the variable $z_k = e^{j(2\pi k/\ell\Delta t)}$ $(k = 0, 1, \ldots, \ell - 1)$ corresponds to the frequency points at $2\pi k/\ell\Delta t$ with Δt being the sampling time interval and ℓ the length of data. The factorization in Eq. (32) is not unique. For convenience and simplicity, one can choose the orders of both polynomials to be $p - 1$.

Premultiplying Eq. (32) by $\alpha(z_k)$ produces

$$\alpha(z_k)G(z_k) = \beta(z_k) \tag{34}$$

which can be rearranged into

$$\begin{aligned}&\alpha_0 G(z_k) + \alpha_1 G(z_k) z_k^{-1} + \cdots + \alpha_{p-1} G(z_k) z_k^{-(p-1)} \\ &\quad = \beta_0 + \beta_1 z_k^{-1} + \cdots + \beta_{p-1} z_k^{-(p-1)}\end{aligned} \tag{35}$$

Equation (35) is the z transform of Eq. (2). With $G(z_k)$ and z_k^{-1} known, Eq. (35) is a linear equation. Because $G(z_k)$ is known at $z_k = e^{j(2\pi k/\ell\Delta t)}$ $(k = 0, \ldots, \ell - 1)$, there are ℓ equations available. Stacking up the ℓ equations yields

$$\Theta\Phi = 0_{m \times \ell} \tag{36}$$

where

$$\Phi = \begin{bmatrix} G(z_0) & G(z_1) & \cdots & G(z_{\ell-1}) \\ G(z_0)z_0^{-1} & G(z_1)z_1^{-1} & \cdots & G(z_{\ell-1})z_{\ell-1}^{-1} \\ \vdots & \vdots & \ddots & \vdots \\ G(z_0)z_0^{-(p-1)} & G(z_1)z_1^{-(p-1)} & \cdots & G(z_{\ell-1})z_{\ell-1}^{-(p-1)} \\ I_r & I_r & \cdots & I_r \\ z_0^{-1}I_r & z_1^{-1}I_r & \cdots & z_{\ell-1}^{-1}I_r \\ \vdots & \vdots & \ddots & \vdots \\ z_0^{-(p-1)}I_r & z_1^{-(p-1)}I_r & \cdots & z_{\ell-1}^{-(p-1)}I_r \end{bmatrix} \tag{37}$$

$$\Theta = [-\alpha_0 \quad -\alpha_1 \quad \cdots \quad -\alpha_{p-1} \quad \beta_0 \quad \beta_1 \quad \cdots \quad \beta_{p-1}]$$

Note that Φ is an $(m + r)p \times (r\ell)$ matrix and Θ an $m \times (m + r)p$ matrix. Equation (36) is a linear algebraic equation, implying that the parameter matrix Θ is in the column null space of Φ. The column null space of Φ is identical to the column null space of $\Phi\Phi^*$ where $*$ is complex conjugate and transpose. Postmultiplying Eq. (36) yields

$$\Theta\bar{\mathcal{R}} = 0_{m \times p(m+r)} \tag{38}$$

where

$$\bar{\mathcal{R}} = \Phi\Phi^* \tag{39}$$

The zero matrix $0_{m \times p(m+r)}$ of dimension $m \times p(m + r)$ in Eq. (38) is, in general, much smaller than $0_{m \times \ell}$ in Eq. (36). It is easy to compute $\Phi\Phi^*$ without fully forming out the matrix Φ, due to its special configuration. It is much easier to compute Θ from Eq. (38) than from Eq. (36).

Equation (38) is identical in form to Eq. (11) except that $\bar{\mathcal{R}}$ in Eq. (38) is a complex matrix whereas $\mathcal{R}$ in Eq. (11) is a real matrix. Both Eqs. (11) and (38) are derived to solve for ARX coefficient matrices α and β. Both α and β are real matrices. Therefore, $\mathcal{R}$ and $\bar{\mathcal{R}}$ should have common properties. Since $\bar{\mathcal{R}}$ is a Hermitian matrix, i.e., $\bar{\mathcal{R}} = \bar{\mathcal{R}}^*$, the real part of $\bar{\mathcal{R}}$ is a symmetric matrix and the imaginary part of $\bar{\mathcal{R}}$ is a skew symmetric matrix. It becomes intuitive to suggest that the real part of $\bar{\mathcal{R}}$ be considered as $\mathcal{R}$, i.e.,

$$\mathcal{R} = \text{real part of } [\bar{\mathcal{R}}] = \text{real part of } [\Phi\Phi^*] \tag{40}$$

As soon as the real matrix $\mathcal{R}$ is computed, it can be used exactly the same way as in the time domain for identification of a system model. In other words, the time-domain methods such as OKID and SRIM can be readily applied. The matrix $\mathcal{R}$ from Eq. (40) is called the frequency-domain information matrix.

Although the matrix $\mathcal{R}$ defined in Eq. (40) is constructed for computing the ARX coefficient matrices, it may also be used for calculating the state matrix A and the output matrix C. Similar to the partition shown in Eq. (12), let $\mathcal{R}$ be partitioned into four parts, i.e.,

$$\mathcal{R} = \begin{bmatrix} \mathcal{R}_{11} & \mathcal{R}_{12} \\ \mathcal{R}_{12}^T & \mathcal{R}_{22} \end{bmatrix} \tag{41}$$

where $\mathcal{R}_{11}$ is a $pm \times pm$ square matrix, $\mathcal{R}_{12}$ a $pm \times pr$ rectangular matrix, and $\mathcal{R}_{22}$ a $pr \times pr$ square matrix. Now, consider the following conceptual equalities:

$$\mathcal{R}_{11} \equiv \mathcal{R}_{yy}, \qquad \mathcal{R}_{12} \equiv \mathcal{R}_{yu}, \qquad \text{and} \qquad \mathcal{R}_{22} \equiv \mathcal{R}_{uu} \tag{42}$$

The $pm \times pm$ matrix $\mathcal{R}_{hh}$ defined in Eq. (9) can be formed as

$$\mathcal{R}_{hh} = \mathcal{R}_{11} - \mathcal{R}_{12}\mathcal{R}_{22}^{-1}\mathcal{R}_{12}^{T} \tag{43}$$

The matrix $\mathcal{R}_{hh}$ can be used by the SRIM algorithm to determine A and C. On the other hand, the matrix product $\mathcal{R}_{12}\mathcal{R}_{22}^{-1}$ (or $\mathcal{R}_{yu}\mathcal{R}_{uu}^{-1}$) can be used by either the direct method or indirect method to determine the input matrix B and the transmission matrix D.

A. Transfer-Function-Error Minimization Method

The indirect and direct methods shown in Ref. 12 for computing B and D do not necessarily minimize the error between the real transfer function and estimated transfer function when truncation of small SVs is involved in computing A and C. Similar to the OEM method[12] in the time domain, the transfer-function-error minimization method forms an equation that explicitly relates the transfer function to B and D with given A and C.

The $m \times r$ transfer function $G(z_k)$ shown in Eq. (32) has another form of expression in terms of system matrices

$$G(z_k) = D + C(z_k I_n - A)^{-1}B \tag{44}$$

for all z_k ($k = 0, 1, \ldots, \ell - 1$). Equation (44) produces

$$\begin{bmatrix} G(z_0) \\ G(z_1) \\ \vdots \\ G(z_\ell - 1) \end{bmatrix} = \begin{bmatrix} I_m & C(z_0 I_n - A)^{-1} \\ I_m & C(z_1 I_n - A)^{-1} \\ \vdots & \vdots \\ I_m & C(z_{\ell-1} I_n - A)^{-1} \end{bmatrix} \begin{bmatrix} D \\ B \end{bmatrix} \tag{45}$$

where I_m and I_n are identity matrices of order m and n, respectively. Given A, C, and $G(z_k)$, matrices D and B can then be determined as follows:

$$\begin{bmatrix} D \\ B \end{bmatrix} = \begin{bmatrix} I_m & C(z_0 I_n - A)^{-1} \\ I_m & C(z_1 I_n - A)^{-1} \\ \vdots & \vdots \\ I_m & C(z_{\ell-1} I_n - A)^{-1} \end{bmatrix}^{\dagger} \begin{bmatrix} G(z_0) \\ G(z_1) \\ \vdots \\ G(z_\ell - 1) \end{bmatrix} \tag{46}$$

For noisy systems, the solutions D and B do not satisfy Eq. (45) but rather minimize the error in the least-square sense between the left-hand side and the right-hand side of Eq. (45). In practice, only the real part of Eq. (45) is needed for the determination of D and B.

B. Experimental Example

This example uses experimental data taken from a large-truss-type structure. The structure shown in Fig. 2 is a NASA testbed that has been used to study controls-structures interaction problems.[17] The system has eight pairs of collocated inputs and outputs for control. The inputs are air thrusters and the outputs are accelerometers. The locations of the input–output pairs are depicted in Fig. 2. The structure was excited using random input signals to four thrusters located at positions 1, 2, 6, and 7. The input and output signals were filtered using low-pass digital filters with the range set to 78% of the Nyquist frequency (12.8 Hz) to concentrate the energy in the low-frequency range below 10 Hz. A total of 2048 data points at a sampling rate of 25.6 Hz from each sensor is used for identification. In this example, four FRFs from two input and output pairs located at positions 1 and 2 are simultaneously used to identify a state-space model of the system.

The integer $p = 50$ is sufficient to identify as many as 50 modes (a system of dimension 100). A state-space model is obtained using the frequency-domain version of SRIM with the system order truncated to 80 by SVs truncation and then further reduced to 78 by eliminating an unstable mode. The reconstructed frequency response data (dashed lines) are compared with the experimental data (solid lines) in Fig. 3.

Figure 3 is the frequency response of output 1 with respect to input 1, representing a case of a strong signal. The reconstructed FRF is obtained using the identified system matrices A, B, C, and D, where C and D are computed by the indirect method. There

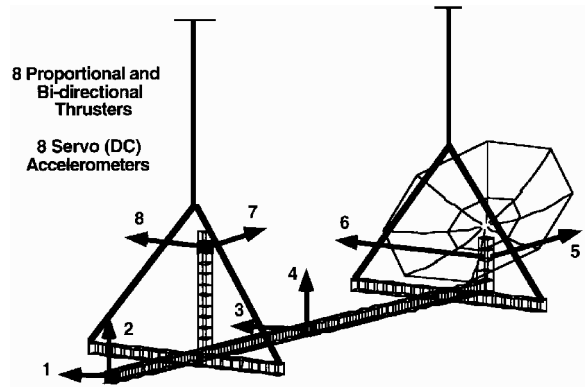

Fig. 2 NASA large-space-structure testbed.

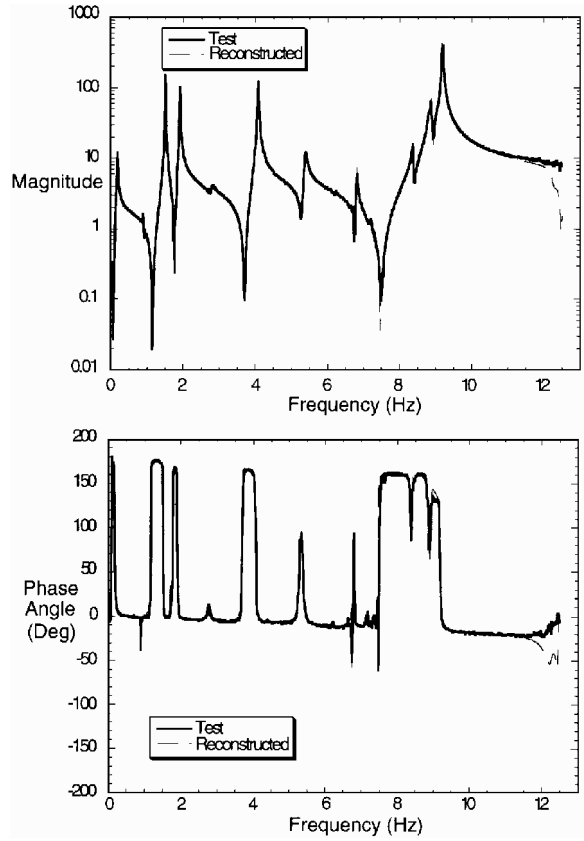

Fig. 3 Comparison of the test and reconstructed input-1/output-1 FRFs; reconstructed FRF is obtained using the identified system matrices.

are 33 modes (corresponding to 66 states) with damping less than 1%. The largest SV of the transfer-function error between the test and reconstructed FRFs is 128.89. Careful examination of Fig. 3 reveals that there are some noticeable discrepancies near the right endpoints of both the magnitude and phase plots. One way to fix the discrepancy is to recompute B and D using the transfer-function-error minimization method. Figure 4 shows the frequency response of output 1 with respect to input 1 using the newly computed B and D. The transfer-function error is reduced from 128.89 to 65.184. There is clearly a tradeoff, i.e., the discrepancy between the test and reconstructed FRFs in Fig. 3 has been moved from the end to somewhere around 8 Hz in Fig. 4.

Similar results (not shown) have been obtained for other input–output pairs. The frequency response of output 2 with respect to input 1 represents the case of a weak signal. The signal is weak because sensor 2 is orthogonal to input 1. The results show that the matching is better for the strong signal cases.

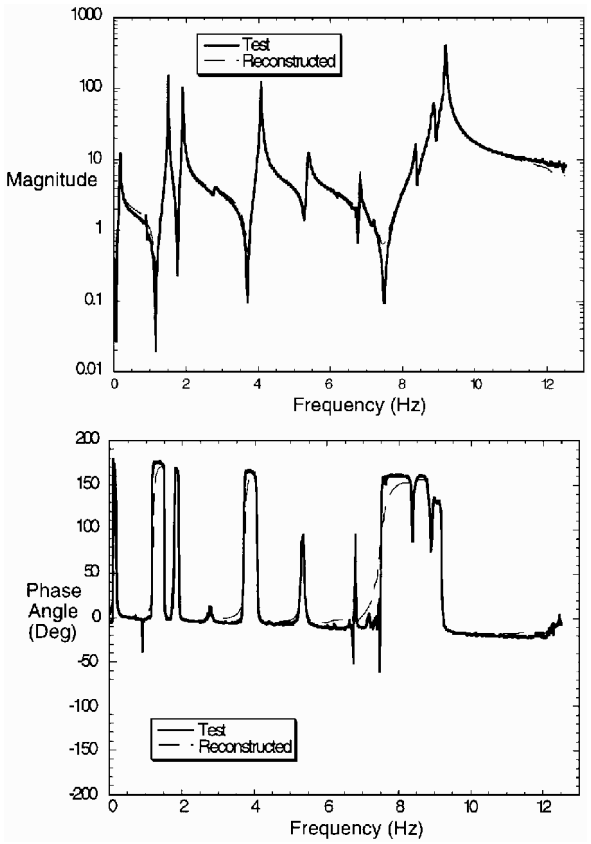

Fig. 4 Comparison of the test and reconstructed input-1/output-1 FRFs; matrices *B* and *D* are computed from transfer-function-error minimization method.

Concluding Remarks

The main contribution of this paper is to unify several system realization algorithms. Other contributions include the introduction of the information matrix in the frequency domain and the development of the frequency-domain version of these realization algorithms. The idea of data correlation leads to establishing the relationship among several system realization algorithms. The approach of using the information matrix provides a way to better understand and interpret these algorithms. Indeed, the information matrix is the common ground for computing system matrices. Some methods use the basis vectors of the column space of the information matrix to determine system matrices. Other methods use the basis vectors of the column null space of the information matrix to calculate system matrices. Both approaches should produce identical results in theory. However, identification results may be noticeably different in practice due to system uncertainties and measurement noises, as evidenced by the experimental examples given. For a pulse or free-decay response, the information matrix reduces to the shifted output data correlation matrix. It implies that the unification includes the classical realization methods using pulse response data. The mathematical unification presented should help users to interpret the identification results obtained from different methods.

References

[1]Juang, J.-N., *Applied System Identification*, Prentice–Hall, Englewood Cliffs, NJ, 1994.

[2]Allemang, R. J., Brown, D. L., and Fladung, W., "Modal Parameter Estimation: A Unified Matrix Polynomial Approach," *Proceedings of the 12th International Modal Analysis Conference* (Honolulu, HI), Society of Experimental Mechanics, Bethel, CT, 1994, pp. 501–514.

[3]Juang, J.-N., and Pappa, R. S., "A Comparative Overview of Modal Testing and System Identification for Control of Structures," *Shock and Vibration Digest*, Vol. 20, No. 5, 1988, pp. 4–15.

[4]Denman, E., Hasselman, T., Sun, C. T., Juang, J.-N., Junkins, J. L., Udwadia, F., Venkayya, V., and Kamat M., "Identification of Large Space Structures on Orbit," U.S. Air Force Rocket Propulsion Lab., AFRPL TR-86-054, Edwards AFB, CA, Sept. 1986.

[5]Kung, S., "A New Identification and Model Reduction Algorithm Via Singular Value Decomposition," *12th Asilomar Conference on Circuits, Systems and Computers,* IEEE Computer Society Press, Pacific Grove, CA, 1978, pp. 705–714.

[6]Hollkamp, J. J., and Batill, S. M., "Automated Parameter Identification and Order Reduction for Discrete Series Models," *AIAA Journal,* Vol. 29, No. 1, 1991, pp. 96–103.

[7]Moonen, M., Demoor, B., Vandenberghe, L., and Vandewalle, J., "On- and Off-Line Identification of Linear State-Space Models," *International Journal of Control*, Vol. 49, No. 1, 1989, pp. 219–232.

[8]Moonen, M., and Vandenberghe, L., "QSVD Approach to On- and Off-line State Space Identification," *International Journal of Control*, Vol. 51, No. 5, 1990, pp. 1133–1146.

[9]Verhaegen, M., "Subspace Model Identification: Part 1—The Output-Error State-Space Model identification Class of Algorithms," *International Journal of Control,* Vol. 56, No. 5, 1992, pp. 1187–1210.

[10]Juang, J.-N., Cooper, J. E., and Wright, J. R., "An Eigensystem Realization Algorithm Using Data Correlations (ERA/DC) for Modal Parameter Identification," *Control-Theory and Advanced Technology,* Vol. 4, No. 1, 1988, pp. 5–14.

[11]Juang, J.-N., Phan, M., Horta, L. G., and Longman, R. W., "Identification of Observer/Kalman Filter Markov Parameters: Theory and Experiments," *Journal of Guidance, Control, and Dynamics,* Vol. 16, No. 2, 1993, pp. 320–329.

[12]Juang, J.-N., "System Realization Using Information Matrix," *Journal of Guidance, Control and Dynamics* (to be published).

[13]Juang, J.-N., "State-Space System Realization Using Input/Output Data Correlation," NASA TP 3622, Jan. 97.

[14]Chen, C. W., Juang, J.-N., and Lee, G., "Frequency Domain State-Space System Identification," *Journal of Vibration and Acoustics,* Vol. 116, No. 4,